

1986

# Performance Evaluation of Hermetic Refrigeration Compressor Using Torque Measurement Method

K. Sakitani

J. Koiwa

T. Maekawa

Follow this and additional works at: <https://docs.lib.purdue.edu/icec>

---

Sakitani, K.; Koiwa, J.; and Maekawa, T., "Performance Evaluation of Hermetic Refrigeration Compressor Using Torque Measurement Method" (1986). *International Compressor Engineering Conference*. Paper 528.  
<https://docs.lib.purdue.edu/icec/528>

This document has been made available through Purdue e-Pubs, a service of the Purdue University Libraries. Please contact [epubs@purdue.edu](mailto:epubs@purdue.edu) for additional information.

Complete proceedings may be acquired in print and on CD-ROM directly from the Ray W. Herrick Laboratories at <https://engineering.purdue.edu/Herrick/Events/orderlit.html>

# PERFORMANCE EVALUATION OF HERMETIC REFRIGERATION COMPRESSOR USING TORQUE MEASUREMENT METHOD

<sup>1</sup> K. Sakitani, <sup>1</sup> J. Koiwa, and <sup>2</sup> T. Maekawa

<sup>1</sup> Mechanical Engng. Lab., Daikin Industries Ltd., 1304,  
Kanaoka-cho, Sakai, Osaka

<sup>2</sup> Compressor Dept., Daikin Industries Ltd., 3-12, Chikko-  
shinmachi, Sakai, Osaka

## ABSTRACT

The measurements were performed concerning the shaft torque in the rolling piston-type rotary compressor. In order to measure the shaft torque, the torque sensor technique was proposed. In the present technique, the electromagnetic torque sensor was used and was connected between the motor and the compressor. The validity of the present technique was verified in comparison with the load torque calculated based on the measured data and that predicted using the previous study. It was found that the calculated load torque was good agreement with the predicted one. In addition, the friction torque was evaluated with the torsional two degree of freedom model.

## INTRODUCTION

In response to the need for the variation of heating or cooling capacity with indoor and outdoor air temperature conditions, a heat pump air conditioner having variable speed compressor and fans has been developed for consumer use in Japan. Presently, major concerns with such a heat pump air conditioner are turned to the improvement in seasonal performance to satisfy the energy savings and also compactness of the air conditioner.

Concerning related problems on the rolling piston-type rotary compressor used in the heat pump air conditioner, a few researches on the evaluations of indicated gas power and friction losses operated at various rotating speeds have been undertaken. Sakurai, et al. (1),(2) examined mechanical and indicated efficiencies for various rotating

speeds, and also reported that both efficiencies at higher running speeds were less than at lower speeds. Iwata, et al. (3) investigated friction losses analysis of the rolling piston-type rotary compressor under the various rotating speeds running. In their experiments, they revealed that the fluctuation of the rotating speed in the rolling piston-type rotary compressor enhanced with decreasing the rotating speed.

On the contrary, it is noteworthy that the important issue remains unsettled with regard to the experimental evaluation of shaft torques which is available to carry out the compactness design of the rolling piston-type rotary compressor operating at various speeds. However, there has been no information on shaft torque measured at actual running, while the measured data on shaft torque in hermetic reciprocating compressor operated at constant rotating speed reported by Matsushima, et al. (4).

The objective of the present study is to measure the shaft torque in hermetic rolling piston type rotary compressor. The shaft torque experiment was performed with the measurement technique using the torque meter.

#### SHAFT TORQUE MEASUREMENT

With respect to the shaft torque measurement, the strain gage technique has been reported in the literature (4). The strain gage technique is available for the shaft torque measurement in the compressor driven with sine wave source. However, this technique is inadequate for the measurement in the compressor driven with inverter, since various high harmonics, and hence the reduction of the S/N ratio of the output signal in the strain gage measurement takes place due to the high-frequency noise. The shaft torque results to be reported here were obtained by torsional angle measurements. The torsional angle was measured by using a electromagnetic torque sensor.

#### Testing Apparatus

A schematic diagram of the testing apparatus is presented in Fig.1. The testing apparatus consists mainly of a test compressor, load stand for controlling the operating condition of the compressor and oil circulation stand for controlling oil temperature in a test compressor. As shown in Fig.1, the main components of the load stand includes principally a condenser, an evaporator and a hand expansion valve.

On the other hand, the oil circulation stand was consisted of an oil tank for circulating oil and a oil tank

having a volume of 3000 cm<sup>3</sup>. A sheathed heater of 1.5 kW was inserted in the oil tank for controlling the desired oil temperature. Prior to the runs, the oil circulation stand was operated to provide the desired oil temperature. The control of oil temperature was carried out controlling electric power added to the heater immersed in the oil. And the oil temperature was elevated up to the condensing temperature of the refrigerant to avoid the condensation of discharge gas in the vessel.

Detail of the test compressor is depicted in Fig.2. As illustrated in Fig.2, the test compressor is consisted of the cylindrical pressure vessel and the compressor unit having a torque measurement device. In the compressor unit, a rolling piston-type rotary compressor with a displacement volume of 10. cc/rev was modified for measuring the shaft torque.

To facilitate the shaft torque studies, a torque sensor was installed between the compressor and a motor, and also was connected with the coupling fabricated with the sufficient torsional stiffness to the motor and the compressor. In addition, to ensure the concentricity between three shafts, each flange of the motor, the torque sensor and the compressor was precisely fabricated, and also was fastened carefully with bolts.

Three piezoelectric pressure transducers were mounted near the suction port, the discharge port and in the compression chamber on the rear cylinder head to measure the dynamic pressures in the cylinder. The absolute pressure in the suction port were determined from the measured dynamic pressure and the static pressure measured using Bourdon tube pressure gage. The absolute pressures in both the discharge port and the compression chamber were also determined using the absolute pressure in suction port.

The torque sensor ( DTP-0.5 type, Ono Sokki Co., ) was used to measure the angle positions. In addition, the digital torque meter ( DTM-408, PD869, Ono Sokki Co., ) was connected to the sensor to convert the angle positions into the shaft torque and the shaft speed. The measurable ranges and the accuracies of the shaft torque and the shaft speed by the sensor were listed in Table 2. With regard to the calibration of the torque sensor, the zero point of output signal from the torque sensor was set at the reading of the torque meter in case that the motor was operated without the compressor. Error of 0.03 %/°C due to the temperature elevation was presented by the testing data of manufacturer, and hence the measurement error in the present runs was approximately within 1.5 %.

As shown in Fig.2, the cylindrical pressure vessel was made of steel, 406 mm of inner diameter, 920 mm of height and 12 mm of thickness. The vessel was divided into four portions, and also was flanged at the ends to facilitate hermetically installation. Moreover, this pressure vessel was designed to make possible to resist a maximum pressure of 2.5MPa under the operation. To endure the vessel, a safety valve of 2.8 MPa was screwed in the upper cover.

In cylindrical wall of pressure vessel, a capillary tube, a suction pipe, a discharge pipe for refrigerant and cable connectors were installed. Cable connectors were provided for the torque sensor leads, the 0.3mm copper-constantan thermocouple leads and the pressure transducers lead. Test compressor was positioned vertically on the lower plate. The pressure vessel was surrounded by the insulation having a sufficient thickness to avoid extraneous heat losses. Thermocouples were embedded in the suction pipe, as indicated in Fig.2, to measure suction gas temperature.

#### Measurement Procedure

After the oil temperature was elevated, up to the condensing temperature, the compressor unit was operated, and also the operating conditions were achieved with the following manner :

- (1) suction pressure was controlled by the hand expansion valve.
- (2) discharge pressure was controlled by supply valve for the cooling water.
- (3) suction gas temperature was maintained by the control of input power added to electric heater in the evaporator.

Under the steady state operating condition, the input power supplied to the compressor was measured using a watt meter. On the other hand, the output signals of the dynamic pressure, and the torque sensor were recorded by an analogue data recorder. In addition, the obtained data on the dynamic pressure, shaft torque and shaft speed were converted a torque diagram using a computer.

#### EVALUATION OF PRESENT MEASUREMENT

The validity of the present shaft torque measurement was verified in comparison with the load torque obtained based on the measured result and that calculated with the mathematical model by Shimizu, et al.(5). To obtain the load torque in the present measurement system, the shaft model was proposed here and the equations on various torques were formulated.

### Proposed Shaft Model

Fig.3 depicts a shaft model used in the present situation to calculate the various kind of torques such as of load, gas compression and friction . In calculating the torques in the present measurement system ( left hand in Fig.3 ), a torsional two degree of freedom model ( right hand ) was proposed.

This model was obtained based on the assumptions that the torsional angles of both the steel couplings could be neglected since the stiffness of both couplings were as same as the stiffness of the shaft. And also the torsional stiffness in measurement shaft equals to that in torque sensor since both the stiffness of motor shaft and compressor shaft are greater in comparison with the stiffness in torque sensor. Table 3 shows the constants on both moments of inertia and stiffness in both the measurement system and model, respectively.

### Load Torque

Using the proposed model, equations of the rotational motion can be given as follows :

$$J_m \ddot{\theta}_m + K_t(\theta_m - \theta_c) = T_m \quad (1)$$

$$J_c \ddot{\theta}_c - K_t(\theta_m - \theta_c) = -T_l \quad (2)$$

where the  $J$  is moment of inertia, the  $\theta$  is angular position, and the  $T$  is torque, respectively. The subscripts of  $m$ ,  $c$  and  $l$  correspond to the motor, the compressor and the load, respectively. The  $K_t$  is torsional stiffness in torque sensor.

In equation (2), the  $T_l$  is calculated using the shaft speed,  $N_c (= 60 \dot{\theta}_c / 2\pi)$ . In both eqs. (1) and (2)  $K_t(\theta_m - \theta_c)$  represents the shaft torque  $T_s$ . Accordingly, the  $T_l$  is determined with  $K_t(\theta_m - \theta_c)$  measured and the  $N_c$  measured.

### Gas Compression Torque

In the present study, the gas compression torque,  $T_g$  is evaluated using pressure  $P_{cc}$ ,  $P_{sc}$  in both compression chamber and suction one, as can be understood in Fig.4. Therefore, the  $T_g$  is expressed as follows :

$$T_g = 11 \ 12 \ h_c ( P_{cc} - P_{sc} ) \quad (3)$$

where the  $11$  is the distance from A to B, the  $12$  is the distance from O to O1 and the  $h_c$  is the cylinder height.

### Friction Torque

The load torque is consisted principally of the gas compression torque,  $T_g$  and the friction torque,  $T_f$  and the oil pumping torque,  $T_o$ . Consequently, the load torque is written by the following equation, since the  $T_o$  is negligible small, compared with the  $T_g$  and the  $T_f$ .

$$T_l = T_g + T_f \quad (4)$$

From equation (4), the  $T_f$  is calculated using both eqs. (2) and (3).

### Powers of Input and Shaft, Motor Efficiency

The input power,  $W_{in}$  of the compressor is evaluated with the reading the watt meter. The shaft power,  $W_{sh}$  is given as :

$$W_{sh} = 9.8 \cdot 2\pi \cdot \overline{T_s} \cdot \overline{N_c} / 60 \quad (5)$$

where the  $\overline{N_c}$  is the average shaft speed and the  $\overline{T_s}$  is the average shaft torque. In this present study, the  $T_s$  is measured with the torque sensor. The motor efficiency,  $\eta_m$  is defined as :

$$\eta_m = W_{sh} / W_{in} \quad (6)$$

## RESULTS AND DISCUSSION

### Measured Dynamic Pressures, Shaft Speed and Shaft Torque

Figs. 5 (a), (b) and (c) show the variations of the pressures, the shaft speed and the shaft torque with time. The origin in the abscissa corresponds to the top dead center.

Fig. 5(a) shows the variations of the dynamic pressures adjacent to suction port and discharge port, and in compression chamber. In this figure, the obtained data of  $P_{sc}$  reveals that the fluctuation of dynamic pressure,  $P_{sc}$  in the present measurement is more significant in comparison with that in the actual case. This is due to the reason that due to the elimination of accumulator the pressure fluctuation remains undamped in the suction process.

Fig. 5(b) shows the variation of the time dependent shaft speed. As seen in Fig. 5(b), the obtained result was found to be superimposed 5th harmonic on first harmonic. The average shaft speed reveals to be about 3440 rpm, and

also the fluctuation of the shaft speed is seen to be lain within  $\pm 100$ rpm.

Fig. 5(c) shows the measured data on the shaft torque. From this figure, it is found that the  $T_s$  reaches at maximum at about 10 msec and also attains a minimum at about 21 msec. In addition, the time at a maximum point of the  $T_s$  corresponds to that a maximum pressure difference between suction chamber pressure,  $P_{sc}$  and compression chamber one,  $P_{cc}$ , as seen in both Fig. 5(a) and 5(c). On the other hand, the 5th harmonic appeared from the maximum  $T_s$  to the minimum  $T_s$  results from the influence of the inertia torque which is caused by the fluctuation of shaft speed. The average  $T_s$  obtained reveals to be 1.54 Nm.

#### Calculated Torque of Shaft, Load, Gas Compression and Friction

Fig.6 illustrates instantaneous data on the various torques against the angular position. In this figure, the  $T_s$ , the  $T_l$ , the  $T_g$  and the  $T_f$  denote the shaft torque, the load torque, the gas compression torque and the friction torque, respectively. The obtained shaft torque curve indicated in Fig. 6 was obtained by tracing successively the arithmetic mean value of the measured data during the divided time interval.

The curve of the  $T_f$  was obtained from eq.(4) and at  $\theta_m = 260^\circ$ , the  $T_f$  shows to attain a maximum. Moreover, it is seen in Fig. 6 that the  $T_l$  curve deviates slightly from the  $T_s$  curve. This difference between the  $T_l$  and the  $T_s$  is presumably due to the fact that the both inertia torque of the piston in the compressor and the gear of torque sensor acts in the present measurement system on the shaft. Comparing the  $T_l$  curve with the  $T_g$  curve in Fig. 6, it is clear that both difference is small. From such a measurement finding, it is evident that the friction torque in the rolling piston-type rotary compressor become small.

#### Predicted Torque of Load, Gas Compression Friction

Fig. 7 shows the torques data predicted using the proposed analysis. Inspecting this figure, it is apparent that the predicted data on the  $T_l$ , the  $T_g$  and the  $T_f$  is good agreement with the measured data. Therefore, it is confirmed that the present measurement of the shaft torque and the proposed model to evaluate the load torque, the gas compression torque and the friction torque are available.

#### Comparison of Measured Data with Cited Data

Fig. 8 depicts the comparisons of the present results of the motor efficiency,  $\eta_m$ , and the input power,  $W_{in}$  with the cited data (manufacturer). The abscissa of the figure



represents the evaporating temperature, Teva, of R-22. In motor efficiency, the present results calculated with the measured data lie slightly below the cited data by the motor manufacturer. On the contrary, the measured data on the input power to the compressor become higher than the cited data by the compressor manufacturer. It might be considered that this was caused by the increased oversuction loss which was induced by the increase of the pressure fluctuation.

#### CONCLUSIONS

In the present study, the shaft torque measurement was discussed and was carried out using the torque sensor in the hermetic rolling piston-type rotary compressor used widely in the heat pump air conditioner. The torsional angle was measured with the torque sensor to evaluate the shaft torque. In addition, the various torques such as the load torque, the gas compression torque and the friction torque were determined using the proposed model ( 2-degree of freedom ). Validity of the present measurement available was confirmed with the comparison of the calculated data on load torque based on the measured shaft torque and shaft speed with the predicted data.

#### REFERENCES

- (1) E. Sakurai, and J. F. Hamilton, "Measurement of Operating Conditions of Rolling Piston Type Rotary Compressor", Proceedings of the 1982 Purdue Compressor Technology Conference, July 21-23, 1982, pp.60-68.
- (2) E. Sakurai, and J. F. Hamilton, " The Predictional Losses in Variable-Speed Rotary Compressors", Proceedings of the 1984 Purdue Compressor Technology Conference, July 11-13, 1984, pp.331-338.
- (3) H. Iwata, A. Sakazume, and K. Yokoyama, "Loss Analysis of Rolling-Piston Type Speed Controlled Rotary Compressor", Transactions of the JSME (Series B), Vol. 51, No.465, 1985, pp.1736-1741.
- (4) M. Matsushima, and A. Yokoyama, "Studies on Torque Characteristics of Refrigerating Hermetic Compressor", Hitachi Hyoron, Vol. 45, No. 5, 1963, pp.115-120.
- (5) T. Shimizu, T. Shiga, I. Tyuu, "Some Investigation on The Pressure Change Characteristics of A Rotary Compressor", Refrigeration, Vol. 50, No. 573, 1975, pp.7-14.

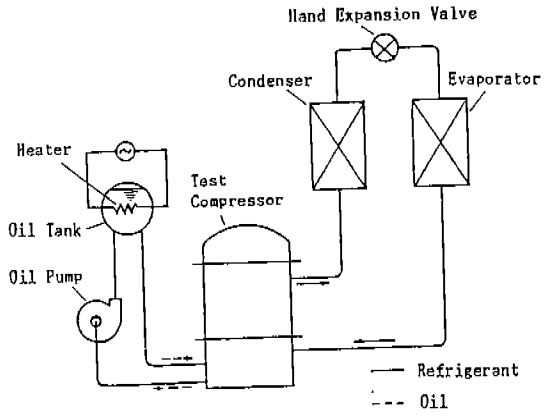


Fig 1 Schematic Diagram of Testing Apparatus

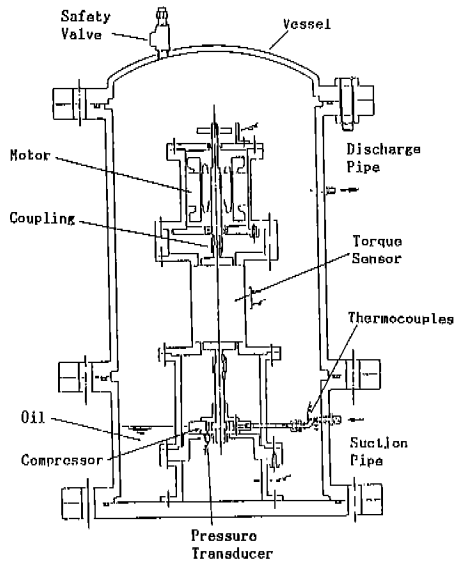
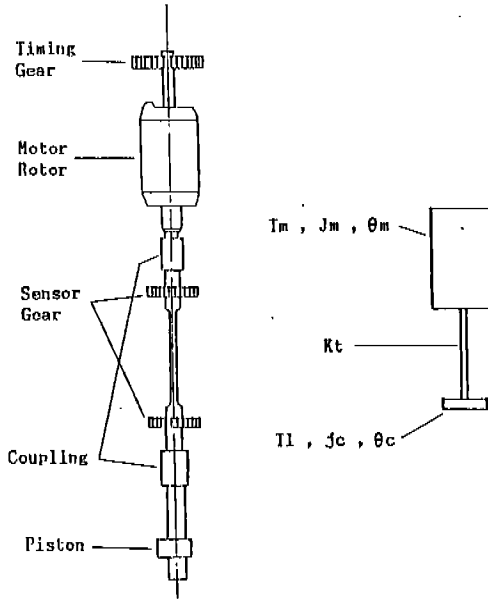


Fig 2 Test Compressor for Measurement

Table 1 Operating Conditions

	No.1	No.2	No.3
Discharge Pressure (MPa)	1.96	1.96	1.96
Suction Pressure (MPa)	.50	.64	.70
Suction Temperature ( C )	20	20	20
Power Source	100 V , 60 Hz		



Measurement System      Model System

Fig 3 Torsional Vibration Model of Test Compressor

Table 2 Measurable Ranges and Accuracies

	Range	Precision
Torque (Nm)	0 - 5	$\pm .09$
Shaft Speed (rpm)	500 - 4000	$\pm 20$

Table 3 Input Data

Moment of Inertia (KG,M <sup>2</sup> )		Stiffness (N.M.S/rad)
Measurement	Model(J <sub>m</sub> ,J <sub>c</sub> )	
Motor Rotor	4.37	250
Timing Gear	1.14	
Sensor Gear	0.80	
Sensor Gear	0.80	
Piston	0.05	
	6.31	
	.85	

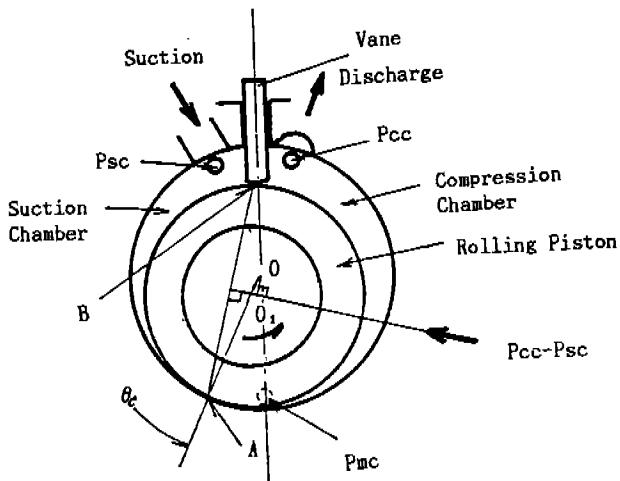
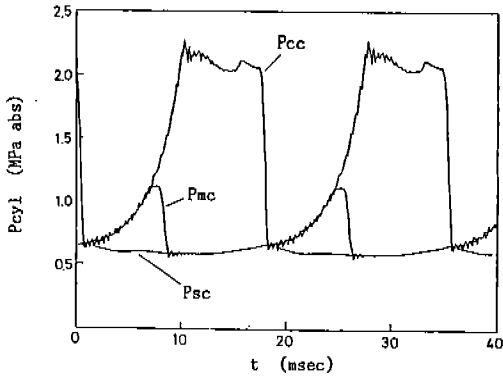
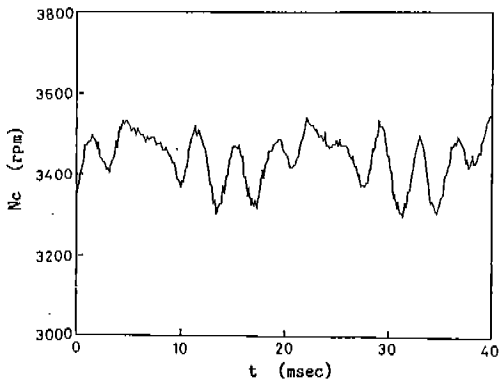


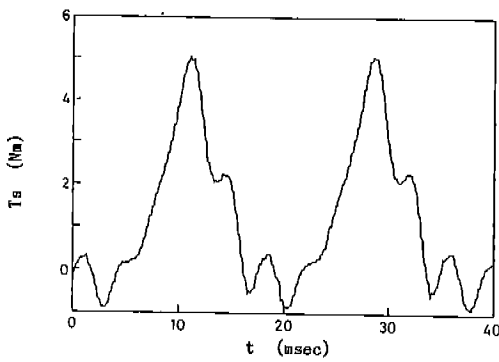
Fig 4 Schematic View of Rolling Piston Type Rotary Compressor



(a)



(b)



(c)

Fig 5 Data on Pressure(a),  
Shaft Speed(b) and Shaft Torque(c)

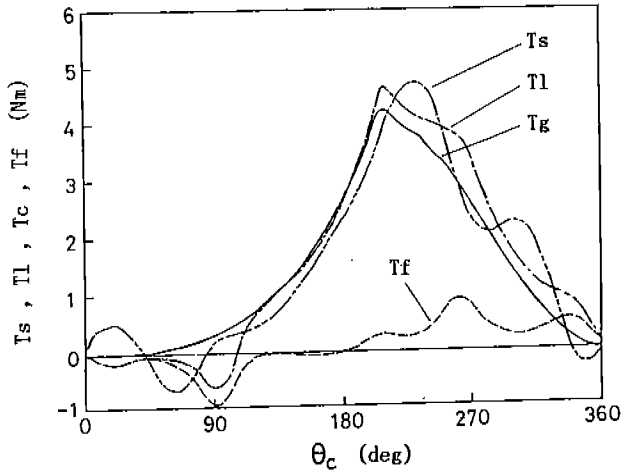


Fig 6 Varius Torques  
(calculated)

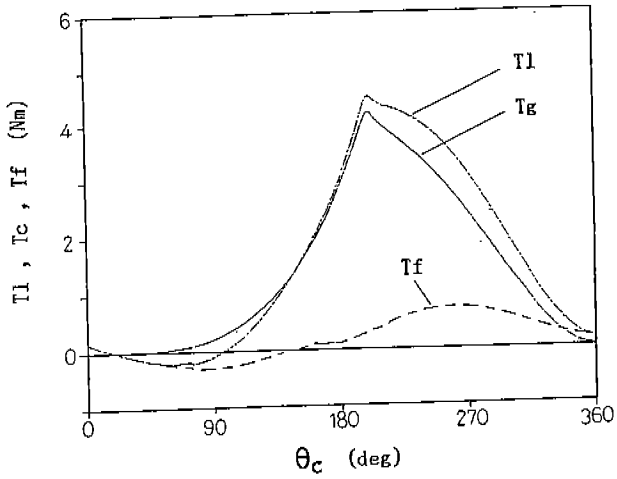


Fig 7 Varius Torques  
(Predicted)

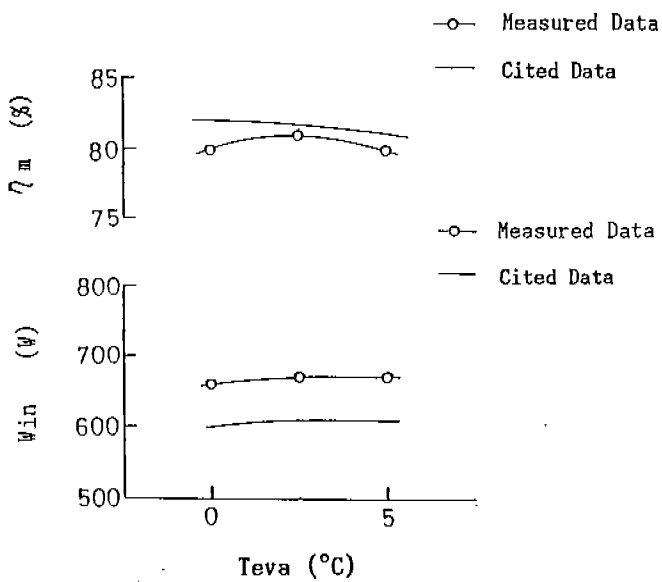


Fig 8 Comparison of Measured Data with Cited Data

PERFORMANCE TESTING OF AN OPEN RECIPROCATING REFRIGERATION  
COMPRESSOR OVER A RANGE OF SPEEDS

James A. McGovern

Department of Mechanical and Manufacturing Engineering,  
Trinity College, Dublin 2, Ireland

ABSTRACT

A load stand has been built and used to determine the performance of an open type reciprocating refrigeration compressor over a range of speeds.

The load stand and instrumentation are described and sample test readings are given. Measured performance characteristics for the compressor over a range of speeds are presented. Aspects of the load stand are discussed and conclusions are drawn from the results of the compressor tests.

SYMBOLS

- $m$  mass flow rate of refrigerant through the compressor, kg/s  
 $Q$  rate of heat transfer in the heat exchanger, W  
 $h_i$  specific enthalpy of refrigerant at measurement location  $i$ , J/kg  
A,B,C,D load stand control valves  
a,b,c,.. measurement locations on the load stand  
M.E.P. mean effective pressure, bar  
TDC top dead centre position  
BDC bottom dead centre position  
 $\eta_{mech}$  mechanical efficiency  
 $\eta_{vol}$  volumetric efficiency